ELSEVIER

Biochimica et Biophysica Acta 1506 (2001) 79–87

BIOCHIMICA ET BIOPHYSICA ACTA
BBA

www.bba-direct.com

Functional coupling of PSST and ND1 subunits in NADH:ubiquinone oxidoreductase established by photoaffinity labeling

Franz Schuler [1], John E. Casida *

Environmental Chemistry and Toxicology Laboratory, Department of Environmental Science, Policy and Management, University of California, 115 Wellman Hall, Berkeley, CA 94720-3112, USA

Received 28 December 2000; received in revised form 17 April 2001; accepted 19 April 2001

Abstract

NADH:ubiquinone oxidoreductase (complex I) is the first, largest and most complicated enzyme of the mitochondrial electron transport chain. Photoaffinity labeling with the highly potent and specific inhibitor trifluoromethyldiazirinyl-[^{3}H]pyridaben ([^{3}H]TDP) labels only the PSST and ND1 subunits of complex I in electron transport particles. PSST is labeled at a high-affinity site responsible for inhibition of enzymatic activity while ND1 is labeled at a low-affinity site not related to enzyme inhibition. In this study we found, as expected, that 13 complex I inhibitors decreased labeling at the PSST site without effect on ND1 labeling. However, there were striking exceptions where an apparent interaction was found between the PSST and ND1 subunits: preincubation with NADH increases PSST labeling and decreases ND1 labeling; the very weak complex I inhibitor 1-methyl-4-phenylpyridinium ion (MPP^+) and the semiquinone analogue stigmatellin show the opposite effect with increased labeling at ND1 coupled to decreased labeling at PSST in a concentration- and time-dependent manner. MPP^+, stigmatellin and ubisemiquinone have similarly positioned centers of highly negative and positive electrostatic potential surfaces. Perhaps the common action of MPP^+ and stigmatellin on the functional coupling of the PSST and ND1 subunits is initiated by binding at a semiquinone binding site in complex I.

Keywords: Photoaffinity labeling; 20 kDa subunit of complex I; 36 kDa subunit of complex I; Rotenone; Stigmatellin; 1-Methyl-4-phenylpyridinium ion; NADH:ubiquinone oxidoreductase

1. Introduction

NADH:ubiquinone oxidoreductase (complex I), the first and most complicated enzyme of the electron transport chain, consists of 42 or 43 subunits [1], seven of which are encoded in the mitochondrial genome and the remainder originate from nuclear DNA [2]. These subunits catalyze the transfer of electrons from NADH to ubiquinone through flavin mononucleotide and at least five iron–sulfur clusters [2]. The catalytic core of complex I may be regarded as the PSST, TYKY, 49 kDa, ND1 and ND5 sub-

Abbreviations: DB, decylubiquinone or 2,3-dimethoxy-5-methyl-6-decyl-1,4-benzoquinone; EPR, electron paramagnetic resonance; ETP, electron transport particle(s); IC_{50}, molar concentration for 50% inhibition; LDH, L-lactate dehydrogenase; MPP^+, 1-methyl-4-phenylpyridinium ion; ND1, 36 kDa subunit of complex I; PSST, 20 kDa subunit of complex I; SDS–PAGE, sodium dodecyl sulfate–polyacrylamide gel electrophoresis; [^{3}H]TDP, tritiated form of trifluoromethyldiazirinyl-pyridaben used as a photoaffinity probe; TPB^-, sodium tetraphenylborate

* Corresponding author. Fax: +1-510-642-6497;
E-mail: ectl@nature.berkeley.edu

[1] Present address: FMC Corporation, Agricultural Products Group, Princeton, NJ 08543, USA.

0005-2728/01/$ – see front matter
PII: S0005-2728(01)00183-9

units [3]. The PSST subunit is proposed to couple electron transfer from iron–sulfur cluster N2 to ubiquinone [4] and ND1 is a candidate subunit to house a ubiquinone binding site [5]. The three-dimensional structure of complex I has been determined only at low resolution [6]. Alternative approaches are necessary to establish the functional relationship between subunits. One of these is photoaffinity labeling in which a potent inhibitor of electron transport is allowed to bind at its high-affinity site where, on exposure to light, it covalently derivatizes the site (e.g. subunit) for characterization.

A serendipitous discovery was made during our studies on photoaffinity labeling of electron transport particles (ETP) with the potent complex I inhibitor trifluoromethyldiazirinyl-[^{3}H]pyridaben ([^{3}H]TDP) (Fig. 1). The [^{3}H]TDP high-affinity labeling site was conclusively identified as being on the PSST subunit and fully accounting for inhibition of enzymatic activity [4]. However, [^{3}H]TDP also labeled a low-affinity site, unrelated to NADH oxidase activity, localized on ND1. [^{3}H]TDP was therefore a potential probe to establish the functional relationship between PSST and ND1. Other complex I inhibitors were accordingly examined with the expected finding that most of them inhibited [^{3}H]TDP labeling of PSST but not ND1. Surprisingly, two respiratory chain inhibitors affected both PSST and ND1, decreasing the labeling of PSST but increasing that of ND1 in an apparently coupled manner. These exceptions were 1-methyl-4-phenylpyridinium ion (MPP^+) (a very weak complex I inhibitor which induces a parkinsonian syndrome [7]) and stigmatellin (a very potent complex III inhibitor and moderately potent complex I inhibitor [8]) with no obvious structural feature in common with the classical complex I inhibitors, e.g. rotenone (Fig. 1). NADH was used to facilitate [^{3}H]TDP binding but unexpectedly increased PSST labeling while decreasing ND1 labeling. This report describes the serendipitous observation of dual and opposing effects on PSST and ND1 and implications on functional coupling between these subunits.

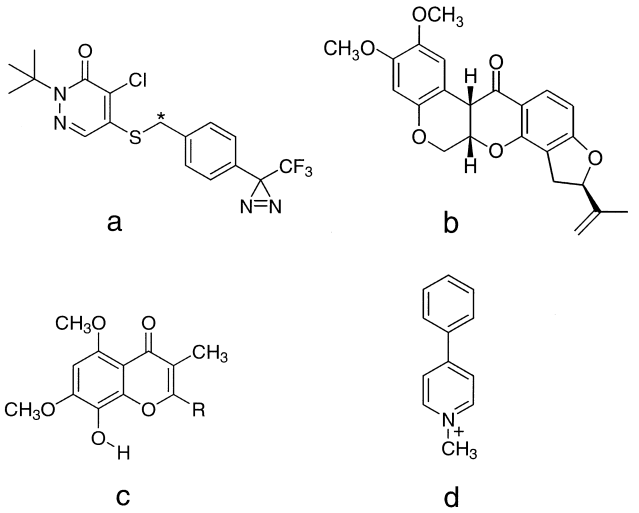

Fig. 1. Main inhibitors used in this study. Trifluoromethyldiazirinyl-[^{3}H]pyridaben (a) is an outstanding photoaffinity probe because it combines exceptional potency as a NADH:ubiquinone oxidoreductase inhibitor (IC_{50} 2.4 nM in the NADH oxidase assay), high specific activity (56 Ci/mmol) and suitable photoreactivity ($t_{1/2}=6$ min under the irradiation conditions used). Rotenone (b), stigmatellin (c) (in which R is a long, unsaturated side chain), MPP^+ (d) and others were used here as inhibitors competing with the binding of (a).

2. Materials and methods

2.1. Materials

ETP were prepared by a described procedure [9]. Protein was determined with the bicinchoninic acid assay (Pierce, Rockford, IL, USA). L-Lactate dehydrogenase (LDH) (type XXXIX, from rabbit muscle) and decylubiquinone (DB) were from Sigma (St. Louis, MO, USA). All inhibitors used were also from Sigma or were available from earlier studies [4,10] except for stigmatellin from Fluka (St. Louis, MO, USA), thiangazole from Syngenta (Basel, Switzerland), tebufenpyrad from American Cyanamid (Parsippany, NJ, USA) and fenpyroximate from Nihon Nohyaku (Osaka, Japan). Synthesis of [^{3}H]TDP (56 Ci/mmol) is described by Latli et al. [11]. MPP^+ was prepared by *N*-methylation of 4-phenylpyridine with excess iodomethane [12] in acetonitrile and recrystallized from ethanol to a purity of $>95\%$.

2.2. Enzyme activity assays

Inhibition of NADH:ubiquinone oxidoreductase was determined by the NADH oxidase and NADH:quinone reductase assays [13]. For the NADH oxidase assay, ETP (20 μg protein) were incubated with

the inhibitor in 990 μl buffer (250 mM sucrose, 50 mM sodium phosphate, pH 7.5) for 5 min at 30°C. Residual activity was determined by addition of NADH (200 μM final concentration) in 0.1% sodium bicarbonate (10 μl) and monitoring for 2 min at 340 nm. The NADH oxidase procedure was varied in all studies with MPP^+ as follows: ETP (100 μg protein) incubated with MPP^+ (0–20 mM) in 1 ml buffer for 5–100 min at 25°C, then NADH added (400 μM final concentration) with monitoring for 1 min at 340 nm. Each assay was performed in triplicate; the control activity of the ETP preparation used was 2.3 ± 0.1 μmol NADH/min/mg ETP at 30°C. The NADH:quinone reductase assay was performed using ETP (40 μg protein) incubated with the inhibitor (0–20 mM) and NADH (200 μM) in 990 μl buffer as above containing 2 mM potassium cyanide and 2 μM antimycin A for 5–30 min at 30°C. The assay was started by addition of DB (100 μM final concentration) in ethanol (10 μl) and monitored for 2 min at 340 nm; the control activity for this assay was 0.53 ± 0.05 μmol NADH/min/mg ETP. IC_{50} values (molar concentrations for 50% inhibition) were determined by iterative nonlinear least-square regression using the SigmaPlot software (SPSS, Chicago, IL, USA).

2.3. Photoaffinity labeling

ETP (300 μg protein) were incubated with the inhibitor in buffer (3 ml) as above. Next, [^{3}H]TDP (8–100 nM final concentration) was added in ethanol (10 μl) followed by incubation for 5–100 min. Then, NADH or NAD (400 μM final concentration), DB (0 or 30 μM, added in 10 μl ethanol) and sodium pyruvate (1 mM final concentration, introduced in buffer) were added and incubated for 10 min at 25°C. Immediately before photochemical activation of [^{3}H]TDP, residual NADH ($\varepsilon_{max}^{340} = 6.22$ mM^{-1} cm^{-1}) was oxidized using LDH (3 units) so that it would not quench the UV light and thereby prevent photoaffinity labeling. Samples were then irradiated for 30 min at 10°C in a Rayonet photochemical reactor equipped with a merry-go-round apparatus and six RPR-3500A lamps. Proteins were pelleted (12 min, $144\,000 \times g$, 4°C) for analysis by 13.5% sodium dodecyl sulfate–polyacrylamide gel electrophoresis (SDS–PAGE), cutting in 2 mm slices and liquid scintillation counting as previously described [4]. Fluorographic analysis of ^{3}H-labeled proteins separated by SDS–PAGE was performed with Amplify on Hyperfilm MP (Amersham Pharmacia Biotech, Piscataway, NJ, USA) according to the manufacturer's instructions.

Significant differences among the groups were determined by one-way analysis of variance followed by Bonferroni's method.

2.4. Molecular modeling

Density functional calculations based on Becke-Perdew (referred to as BP86) [14] were made for analogues of stigmatellin and ubisemiquinone (methyl replacing the long unsaturated side chain) and for MPP^+ on the DN** basis set. The electrostatic potential surfaces were then generated by mapping the density functionals onto electron density surfaces (0.002 electron/Å) using the program SPARTAN (Spartan 5.1, Wavefunction, Irvine, CA, USA).

3. Results

3.1. Effects of NADH and decylubiquinone on [^{3}H]TDP labeling of PSST and ND1

The effects were examined of NADH, NAD and DB on [^{3}H]TDP labeling of the two subunits (Fig. 2). The [^{3}H]TDP level used (80 nM) gave similar labeling of PSST and ND1 in the controls with no cofactor or substrate. The basal levels of PSST and ND1 labeling were unaffected or not greatly changed by NAD or DB alone or together. In contrast, NADH increased PSST labeling and decreased ND1 labeling significantly (Fig. 2) with no apparent effect of DB on this labeling.

3.2. Effects of respiratory chain inhibitors on NADH:quinone reductase activity and on [^{3}H]TDP labeling of PSST and ND1

Seventeen compounds were examined for inhibitory effects on enzyme activity and [^{3}H]TDP labeling of PSST and ND1 (Table 1). All of the compounds are primarily complex I inhibitors except myxothiazol and stigmatellin, which are more potent on complex III than I, and antimycin A which is only a

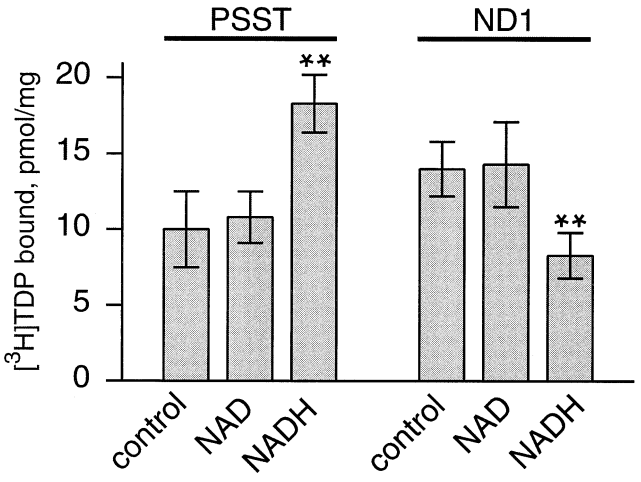

Fig. 2. Effects of cofactors on [^{3}H]TDP labeling of PSST and ND1. ETP (300 μg protein) in sucrose-phosphate buffer pH 7.5 (3 ml) were labeled with [^{3}H]TDP (80 nM) in the presence or absence of the cofactors NAD or NADH (400 μM) and DB (30 μM). DB showed no effect on labeling of PSST and ND1 in controls or with NAD or NADH and was therefore not considered a variable in presenting this figure or in the data analysis. **Highly significant difference ($P < 0.01$) compared with the control ($n = 4$).

complex III inhibitor. Nine potent complex I inhibitors (including rotenone, piericidin A and bullatacin) at 2 μM almost completely block PSST labeling without greatly affecting ND1 labeling. Four moderately potent complex I inhibitors (papaverine, capsaicin, 4-phenylpyridine and myxothiazol at 30–300 μM) give 42–66% labeling of PSST with normal ND1 labeling. Of all the inhibitors, only myxothiazol (30 μM) precipitated the ND1 subunit apparent by streaking on SDS–PAGE with corresponding diffusion of the labeled 30 kDa region. Antimycin A and amobarbital (a very weak complex I inhibitor) at the concentrations used did not affect either PSST or ND1 labeling. Thus, these 15 respiratory inhibitors have little or no effect on ND1 labeling. However, two compounds gave the very surprising result of lowering PSST labeling to 35–49% while elevating ND1 labeling to 175–200% of the control. MPP^+ and stigmatellin are therefore of special interest since they simultaneously but oppositely affect labeling of the two subunits. Fig. 3 illustrates the marked difference in [^{3}H]TDP labeling of PSST and ND1 in the presence of rotenone and MPP^+, i.e. rotenone inhibits PSST labeling without effect on ND1 while MPP^+ inhibits PSST and elevates ND1 labeling.

3.3. Correlation of MPP^+-induced inhibition of [^{3}H]TDP labeling of PSST and NADH oxidase activity

MPP^+ at 0–20 or 30 mM preincubated with ETP for 5 min inhibits PSST labeling and NADH oxidase activity in a concentration-dependent manner (Fig. 4A). Inhibition of PSST labeling correlated well with inhibition of NADH oxidase activity (with correlation coefficients of 0.92 and 0.84 at 8 nM and 80 nM [^{3}H]TDP, respectively; data not shown). The ion-pairing agent tetraphenylborate (TPB^-) uncouples inhibition of NADH oxidase activity by MPP^+ from its inhibition of labeling at PSST. Repetition of the experiment shown in Fig. 4A in the presence of TPB^- (10 μM) led to the expected strong increase in the potency of MPP^+ as an inhibitor of NADH oxidase, i.e. enzymatic activity of complex I is fully

Table 1
Effects of respiratory chain inhibitors on NADH:quinone reductase activity and on [^{3}H]TDP labeling of PSST and ND1

Inhibitor (μM)	Enzyme activity IC_{50} (nM)	Labeling (%)	
		PSST	ND1
No effect on ND1 labeling			
Pyridaben (2)	11	< 5	98
Rotenone (2)	12	< 5	96
Piericidin A (2)	25	< 5	93
Bullatacin (2)	2.9	< 5	93
Rolliniastatin I (2)	3.0	< 5	97
Fenpyroximate (2)*	1.2	< 5	72
Tebufenpyrad (2)*	180	< 5	88
Thiangazole (2)*	50	< 5	95
Fenazaquin (2)*	190	19	92
Papaverine (300)*	36 000	42	100
Capsaicin (300)*	86 000	46	96
4-Phenylpyridine (300)*	42 000	65	89
Myxothiazol (30)	3 000	66	110
Antimycin A (30)	> 100 000	94	117
Amobarbital (3000)*	1.2 mM	107	95
Elevation of ND1 labeling			
MPP^+ (20 000)	0.9 mM	35	200
Stigmatellin (30)	> 30 000	49	175

Enzyme activity IC_{50} values are for 5 min preincubation of enzyme and inhibitor before NADH:quinone reductase assay as described in Section 2. For labeling, ETP (300 μg protein in 3 ml sucrose-phosphate buffer pH 7.5) were treated sequentially with the inhibitor, [^{3}H]TDP (80 nM) and NADH (400 μM) each for 10 min followed by SDS–PAGE analysis as in Fig. 3B. Labeling results are mean values from 2–5 experiments except for single experiments indicated by an asterisk.

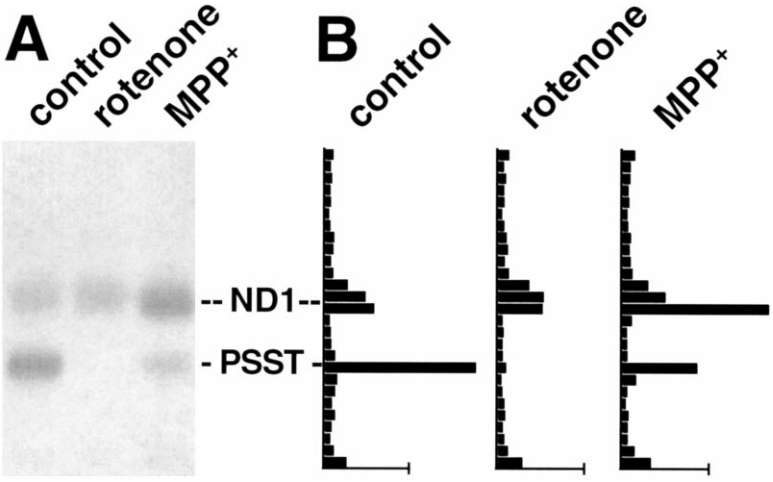

Fig. 3. Effects of rotenone and MPP^+ on [^{3}H]TDP labeling of PSST and ND1. (A) Fluorogram illustrating labeling of PSST and ND1 in untreated ETP (control), the inhibition of PSST but not ND1 labeling by rotenone, and the inhibition of PSST and elevation of ND1 labeling by MPP^+. (B) Quantitation of gel slices corresponding to fluorogram. ETP (300 μg protein) in sucrose-phosphate buffer pH 7.5 (3 ml) were incubated for 30 min at 25°C in buffer alone (control) or with rotenone (2 μM) or MPP^+ (20 mM) then photoaffinity labeled with [^{3}H]TDP (80 nM) in the presence of NADH (400 μM). Each calibration bar at the bottom designates 1×10^6 dpm/mg protein; control values for labeling (pmol [^{3}H]TDP/mg protein) are 12 ± 2 for PSST and 9.7 ± 3.4 for ND1 ($n=8$).

blocked by 20 mM MPP^+ in the presence of 10 μM TPB^- (Fig. 4B) whereas, without the ion-pairing agent, NADH oxidase activity is only reduced by 40% (Fig. 4A). However, the presence of TPB^- did not affect the degree of [^{3}H]TDP displacement at PSST by MPP^+ (Fig. 4B).

3.4. Effects of MPP^+ on [^{3}H]TDP labeling of ND1

3.4.1. Heat instability confirms ND1 as the site of MPP^+-elevated [^{3}H]TDP labeling of ETP

Heat denaturation (100°C) of isolated complex I in SDS–PAGE buffer leads to precipitation of the very hydrophobic ND1 subunit [15]. This heat instability was used to test whether the increase in [^{3}H]TDP binding at 30 kDa (the position of ND1) with 20 mM MPP^+ was indeed at this complex I subunit. Denaturation of labeled complex I (isolated by Blue Native PAGE [16]) or labeled ETP in SDS sample buffer at 100°C (4 min) resulted in 60% lower recovery of the original radioactivity at the ND1 site than at the PSST site. This is consistent with the MPP^+-elevated labeling being on the heat-sensitive ND1.

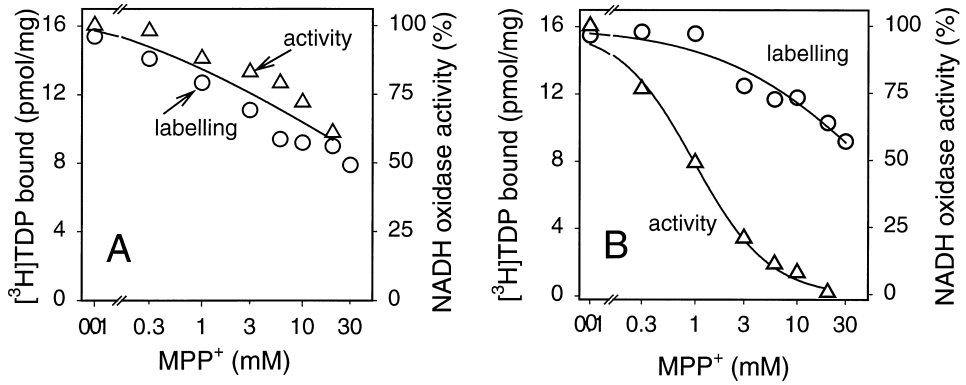

Fig. 4. MPP^+-induced inhibition of [^{3}H]TDP labeling of PSST and NADH oxidase activity. (A) Concentration-dependent inhibition of labeling and enzymatic activity. ETP (100 μg protein/ml) were incubated with MPP^+ for 5 min at 25°C and then labeled with [^{3}H]TDP (80 nM). Inhibition of enzymatic activity was determined in parallel experiments. (B) Experiment as in A but in the presence of TPB^- (10 μM).

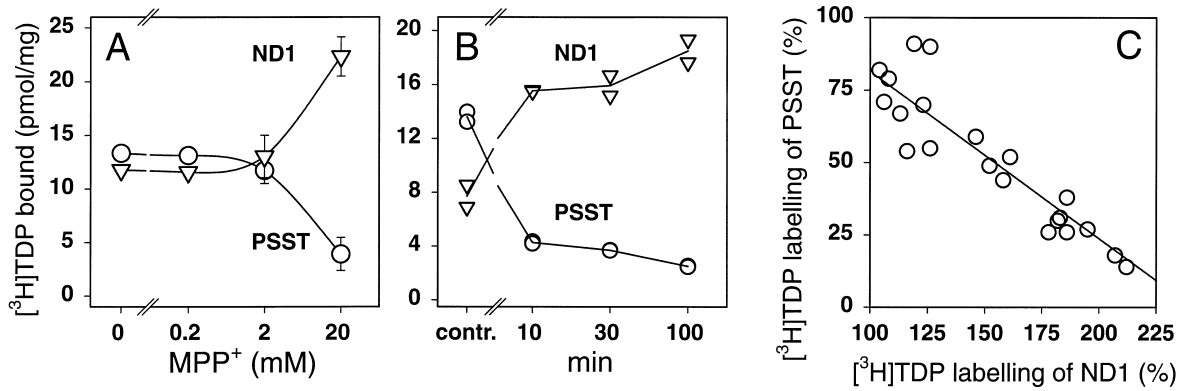

Fig. 5. Effects of MPP^+ concentration and incubation time on [^{3}H]TDP labeling of PSST and ND1. (A) Concentration dependence. ETP (100 μg protein/ml) were incubated with MPP^+ (0, 0.2, 2 or 20 mM) for 30 min at 25°C and then photoaffinity labeled with [^{3}H]TDP (100 nM). (B) Time dependence. ETP (100 μg protein/ml) were incubated with MPP^+ (20 mM) for 10, 30, or 100 min at 25°C followed by photoaffinity labeling with [^{3}H]TDP (80 nM). (C) Elevation of ND1 labeling coupled to decrease of PSST labeling. The data are from panels A and B, from Fig. 4 and supplemental experiments. Each data point represents a labeling experiment in the presence of MPP^+ relative to a control without MPP^+.

3.4.2. *Correlation of MPP^+-induced elevation of ND1 labeling and decrease of PSST labeling*

MPP^+ increases [^{3}H]TDP labeling of ND1 at 20 but not 2 mM (Fig. 5A) and in a time-dependent manner (0–100 min) at 20 mM (Fig. 5B). This is a highly reproducible observation since, at 20 mM MPP^+ with incubation times of 5–100 min, the photoaffinity labeling is significantly increased by a factor of 1.9 ± 0.2 ($n = 10$; $P < 0.005$) compared to controls without inhibitor (data not shown). The MPP^+-induced decrease in PSST labeling is accompanied by an increase in ND1 labeling (Fig. 5A,B). These studies, supplemented with additional experiments of the same type, established a high correlation ($r^2 = 0.84$) between the decrease in PSST labeling and increase in ND1 labeling (Fig. 5C).

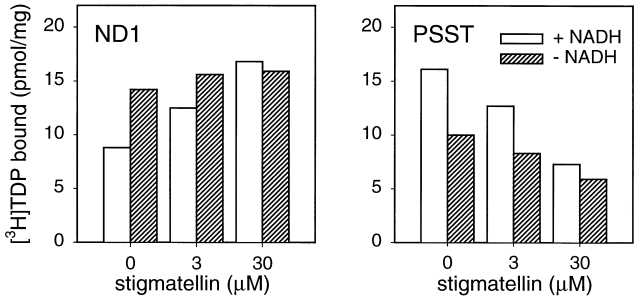

Fig. 6. Effects of stigmatellin on [^{3}H]TDP labeling of ND1 and PSST. ETP (100 μg protein/ml) were labeled with [^{3}H]TDP (80 nM) after incubation for 10 min at 25°C with increasing concentrations of stigmatellin in the presence or absence of NADH. (Left) Labeling of ND1. (Right) Labeling of PSST. Conditions as in Table 1. Typical experiment shown with relationships confirmed in other studies.

3.5. *Effects of stigmatellin on [^{3}H]TDP labeling of PSST and ND1*

Stigmatellin, at concentrations below its IC_{50} value for enzyme activity, was the only compound that mimicked the action of MPP^+ in three respects: partial inhibition of NADH:oxidoreductase activity, decreased labeling of PSST and increased labeling of ND1 (Table 1, Fig. 6). The decrease in labeling of PSST coupled to an increase in labeling of ND1 is dependent on stigmatellin concentration and attenuated by omission of NADH from the incubation (Fig. 6).

3.6. *Common structural features for MPP^+ and stigmatellin*

Stigmatellin, a semiquinone analogue, was compared to ubisemiquinone and MPP^+ by density functional analysis of their electrostatic potential surfaces using standard methods [14]. Although the calculations are not shown, the derived models indicate a close structural similarity between stigmatellin and the protonated ubisemiquinone radical with respect

to similarly positioned centers at about 7 Å distance of highly positive and negative electrostatic potential surfaces. Relative to MPP^+, the positive potential of the polarized methyl group can be compared to the phenolic hydroxyl substituent of stigmatellin and the negative potential surface of the π-electrons in the phenyl ring then mimics the carbonyl oxygen of stigmatellin with the 7 Å distance maintained in all cases (Fig. 1).

4. Discussion

4.1. [^{3}H]TDP labels PSST and ND1

[^{3}H]TDP photoaffinity labels only two proteins in complex I with apparent molecular masses on SDS–PAGE of 23 and 30 kDa, respectively. Labeling of PSST is saturable, correlated with enzyme inhibition and blocked by various structurally unrelated complex I inhibitors. A common binding domain, with partially overlapping sites for inhibitors of many types, was also suggested earlier based on radioligand binding [10,17–19] and fluorescence quenching studies [19]. Labeling of ND1 does not saturate at the [^{3}H]TDP concentrations tested and is not displaced with a number of inhibitors. Rotenone at 2 μM completely prevents [^{3}H]TDP labeling at the PSST site but does not measurably affect photoaffinity labeling of the ND1 subunit. While this suggests that [^{3}H]TDP labeling of ND1 is unspecific it is intriguing to see that ND1, beside PSST, is the sole protein labeled by [^{3}H]TDP in ETP, which likely consists of several hundred protein components. Also, rotenone analogues used as photoaffinity probes with isolated complex I have been shown to label the ND1 site [15,20]. This suggests that both PSST and ND1 have inhibitor binding sites but only action at PSST directly blocks electron transport. Here [^{3}H]TDP is used to characterize the effects on complex I of various cofactors, substrates and inhibitors.

4.2. Effects of NADH and decylubiquinone on [^{3}H]TDP labeling

NADH (but not NAD) elevates [^{3}H]TDP labeling of PSST and lowers labeling of ND1, providing the first direct evidence for coupling between these two subunits. With this finding, NADH was routinely added in the assays. NADH alters the profile of tryptic digestion in isolated complex I [21] and also changes the cross-linking pattern with several reagents between various subunits in isolated complex I [22]. NADH (but not NAD) changes the electron paramagnetic resonance (EPR) signal of iron–sulfur cluster N2 in submitochondrial particles [23] and activates complex I from an inactive to an active state [24]. These effects were rationalized as NADH-induced conformational changes of complex I possibly linked to proton transfer reactions. Activated complex I shows a higher affinity to rotenone than deactivated complex I and the transition from the active to the deactivated state is very slow [24]. In the labeling experiments here, NADH is always oxidized to NAD shortly before irradiation as it would quench the UV light responsible for photoactivation of [^{3}H]TDP. The reported prolonged effects of NADH translate here in the altered [^{3}H]TDP labeling of both ND1 and PSST. DB (30 μM) does not affect [^{3}H]TDP (80 nM) labeling suggesting that either their binding sites do not overlap or that the binding affinity for this quinone is too low to effectively compete with the very potent [^{3}H]TDP.

4.3. Effects of MPP^+ on [^{3}H]TDP labeling

MPP^+-induced parkinsonian syndrome is believed to be related to binding at and inhibition of NADH:ubiquinone oxidoreductase [7], leading to decreased ATP levels [25] and/or increased production of reactive oxygen species [26,27]. MPP^+ prevents binding of [^{14}C]rotenone to complex I [28]. It was surprising to observe that MPP^+ at 20 mM (but not at 1 mM; see [4]) significantly increases [^{3}H]TDP labeling at ND1 while inhibiting PSST labeling. This is in contrast to several other complex I inhibitors which do not alter ND1 labeling. MPP^+-induced inhibition of PSST labeling is concentration- and time-dependent and correlates well with the degree of NADH oxidase inhibition. The time dependence may be related to the charged inhibitor slowly penetrating into the membrane-bound enzyme complex.

Catalytic amounts of the ion-pairing agent TPB^- strongly enhance the potency and kinetics of MPP^+

as a complex I inhibitor perhaps by transporting the ionic inhibitor through the lipid bilayer to a hydrophobic binding site [29]. However, TPB^- does not affect either the MPP^+-induced decrease in [^{3}H]TDP labeling of PSST or increase in labeling of ND1. This apparent anomaly may be explained by two MPP^+-specific binding sites. Binding of MPP^+ to the first, more hydrophilic site affects [^{3}H]TDP labeling of PSST and ND1. TPB^- is needed to shuttle MPP^+ to the second, more hydrophobic site. There, MPP^+ does not interfere with [^{3}H]TDP binding, yet leads to fast and complete block of enzymatic activity. Two MPP^+ binding sites were also suggested by kinetic studies with MPP^+ and its 4′-alkylated analogues [30,31]. It should be stressed that the hydrophobic MPP^+ binding site does not appear to be shared by the classical high-affinity complex I inhibitors.

4.4. Effects of the semiquinone analogue stigmatellin on [^{3}H]TDP labeling

Stigmatellin is a moderately potent inhibitor of NADH:Q_1 reductase activity [8]. The action of MPP^+ at 20 mM was mimicked by stigmatellin at 30 μM with elevated ND1 labeling apparently coupled to inhibition of PSST labeling. This suggests a possible common mode of action. The opposite effects observed for NADH and stigmatellin on [^{3}H]TDP labeling indicate that they induce very different types of conformational changes. Stigmatellin acts as a semiquinone analogue and potently inhibits complex III at the Q_o site [32]. It induces large conformational changes in both complex III [33] and the eukaryotic photosynthetic b_6f complex [34]. A comparison of the electrostatic potential surfaces indicates that the seemingly unrelated MPP^+ and stigmatellin (Fig. 1) fit remarkably well into a pharmacophore of a protonated ubisemiquinone structure. Some complex I inhibitors including 4′-alkyl-MPP^+ analogues have been classified as semiquinone antagonists without direct evidence on their binding sites [35]. Functional models of complex I suggest more than one quinone binding site [36,37] and there are two locally separated semiquinone species observed by EPR in complex I of submitochondrial particles [38,39]. Labeling with [^{3}H]TDP in the presence and absence of TPB^- also suggests two binding sites for MPP^+.

5. Conclusion

[^{3}H]TDP, rotenone and a large number and great variety of potent NADH:ubiquinone oxidoreductase inhibitors bind to a single high-affinity domain in the PSST subunit, leading to a block in the mitochondrial electron transport chain. [^{3}H]TDP also binds to a low-affinity site in ND1 not directly involved in enzyme inhibition and not affected by the majority of complex I inhibitors in competitive binding studies. In contrast, the decreased labeling of PSST in the presence of MPP^+ is coupled to increased labeling of ND1. This unique effect of MPP^+ is only shared by the semiquinone analogue stigmatellin which may suggest that, in contrast to all other inhibitors, these two compounds act in a distinctly different way, possibly as semiquinone analogues at a common binding site also situated – at least partially – in the PSST subunit. Binding of these two compounds may lead to allosteric modification observed as increased labeling of the ND1 subunit. This is the first direct experimental evidence that the PSST and ND1 subunits work together in the coupling reaction between electron transfer and proton transfer. Perhaps, the common binding site for MPP^+ and stigmatellin coincides with the proposed ubiquinone binding site in the PSST – 49 kDa subunit – ND1 region of the catalytic core of complex I [40].

Acknowledgements

This work was supported by funds from the William Muriece Hoskins Chair in Chemical and Molecular Entomology. We thank Gary Quistad and Daniel Schulz-Jander of this laboratory, Kathleen Durkin of the Molecular Graphics Facility (College of Chemistry, University of California at Berkeley) and Takahiro Yano of the University of Pennsylvania Medical Center (Philadelphia, PA) for helpful suggestions.

References

[1] J.M. Skehel, I.M. Fearnley, J.E. Walker, FEBS Lett. 438 (1998) 301–305.
[2] J.E. Walker, Q. Rev. Biophys. 25 (1992) 253–324.

[3] P.M. Ahlers, A. Garofano, S.J. Kerscher, U. Brandt, Biochim. Biophys. Acta 1459 (2000) 258–265.
[4] F. Schuler, T. Yano, S. Di Bernardo, T. Yagi, V. Yankovskaya, T.P. Singer, J.E. Casida, Proc. Natl. Acad. Sci. USA 96 (1999) 4149–4153.
[5] T. Friedrich, M. Strohdeicher, G. Hofhaus, D. Preis, H. Sahm, H. Weiss, FEBS Lett. 265 (1990) 37–40.
[6] N. Grigorieff, J. Mol. Biol. 277 (1998) 1033–1046.
[7] K.F. Tipton, T.P. Singer, J. Neurochem. 61 (1993) 1191–1206.
[8] M. Degli Esposti, A. Ghelli, M. Crimi, E. Estornell, R. Fato, G. Lenaz, Biochem. Biophys. Res. Commun. 190 (1993) 1090–1096.
[9] F.L. Crane, J.L. Glenn, D.E. Green, Biochim. Biophys. Acta 22 (1956) 475–487.
[10] E. Wood, B. Latli, J.E. Casida, Pestic. Biochem. Physiol. 54 (1996) 135–145.
[11] B. Latli, H. Morimoto, P.G. Williams, J.E. Casida, J. Label. Compd. Radiopharm. 41 (1998) 191–199.
[12] B. Emmert, O. Varenkamp, Chem. Ber. 56 (1923) 491–501.
[13] T.P. Singer, in: D. Glick (Ed.), Methods of Biochemical Analysis, vol. 22, Wiley, New York, 1974, pp. 123–175.
[14] E. Wimmer, in: J.K. Labanowski, J.W. Andzelm (Eds.), Density Functional Methods in Chemistry, Springer-Verlag, New York, 1991, pp. 7–33.
[15] F.G.P. Earley, S.D. Patel, C.I. Ragan, G. Attardi, FEBS Lett. 219 (1987) 108–112.
[16] H. Schägger, G. von Jagow, Anal. Biochem. 199 (1991) 223–231.
[17] D.J. Horgan, T.P. Singer, J.E. Casida, J. Biol. Chem. 243 (1968) 834–843.
[18] P.J. Jewess, Biochem. Soc. Trans. 22 (1994) 247–251.
[19] J.G. Okun, P. Lümmen, U. Brandt, J. Biol. Chem. 274 (1999) 2625–2630.
[20] F.G.P. Earley, C.I. Ragan, Biochem. J. 224 (1984) 525–534.
[21] M. Yamaguchi, G.I. Belogrudov, Y. Hatefi, J. Biol. Chem. 273 (1998) 8094–8098.
[22] G. Belogrudov, Y. Hatefi, Biochemistry 33 (1994) 4571–4576.
[23] A.M.Ph. de Jong, A.B. Kotlyar, S.P.J. Albracht, Biochim. Biophys. Acta 1186 (1994) 163–171.
[24] A.D. Vinogradov, Biochim. Biophys. Acta 1364 (1998) 169–185.
[25] T.E. Bates, S.J.R. Heales, S.E.C. Davies, P. Boakye, J.B. Clark, J. Neurochem. 63 (1994) 640–648.
[26] R.R. Ramsay, T.P. Singer, Biochem. Biophys. Res. Commun. 189 (1992) 47–52.
[27] D.S. Cassarino, C.P. Fall, R.H. Swerdlow, T.S. Smith, E.M. Halvorsen, S.W. Miller, J.P. Parks, W.D. Parker Jr., J.P. Bennett Jr., Biochim. Biophys. Acta 1362 (1997) 77–86.
[28] R.R. Ramsay, M.J. Krueger, S.K. Youngster, M.R. Gluck, J.E. Casida, T.P. Singer, J. Neurochem. 56 (1991) 1184–1190.
[29] R.R. Ramsay, R.J. Mehlhorn, T.P. Singer, Biochem. Biophys. Res. Commun. 159 (1989) 983–990.
[30] M.R. Gluck, M.J. Krueger, R.R. Ramsay, S.O. Sablin, T.P. Singer, W.J. Nicklas, J. Biol. Chem. 269 (1994) 3167–3174.
[31] M.J. Krueger, S.O. Sablin, R. Ramsay, T.P. Singer, J. Neurochem. 61 (1993) 1546–1548.
[32] G. von Jagow, T. Ohnishi, FEBS Lett. 185 (1985) 311–315.
[33] H. Kim, D. Xia, C.-A. Yu, J.-Z. Xia, A.M. Kachurin, L. Zhang, L. Yu, J. Deisenhofer, Proc. Natl. Acad. Sci. USA 95 (1998) 8026–8033.
[34] C. Breyton, J. Biol. Chem. 275 (2000) 13195–13201.
[35] M. Degli Esposti, Biochim. Biophys. Acta 1364 (1998) 222–235.
[36] U. Brandt, Biochim. Biophys. Acta 1318 (1997) 79–91.
[37] P.L. Dutton, C.C. Moser, V.D. Sled, F. Daldal, T. Ohnishi, Biochim. Biophys. Acta 1364 (1998) 245–257.
[38] A.D. Vinogradov, V.D. Sled, D.S. Burbaev, V.G. Grivennikova, I.A. Moroz, T. Ohnishi, FEBS Lett. 370 (1995) 83–87.
[39] T. Ohnishi, Biochim. Biophys. Acta 1364 (1998) 186–206.
[40] I. Prieur, J. Lunardi, A. Dupuis, Biochim. Biophys. Acta 1405 (2001) 173–178.